

Case I: $r_0 \leq r_m$ (see Fig. 1)

Starting with (4) we can write

$$\Omega/2 = \int_{\Omega_c'} \int \sin\theta d\theta d\beta \quad (5)$$

where c' is the half-boundary as shown in Figs. 1 and 2. Putting in the limits for θ and β and performing the θ integration we obtain

$$\begin{aligned} \Omega/2 &= \int_0^{\beta_{\max}} \int_0^{\theta_s} \sin\theta d\theta d\beta \\ &= \int_0^{\beta_{\max}} |-\cos\theta|_0^{\theta_s} d\beta \\ &= \beta_{\max} - \int_0^{\beta_{\max}} \cos\theta_s d\beta \end{aligned} \quad (6)$$

where $\theta_s = \angle OPD$, and $\beta_{\max} = \pi$ for $r_0 < r_m$ and $\pi/2$ for $r_0 = r_m$ as can be seen by inspection of Fig. 1. The integral in (6) can be evaluated by writing $\cos\theta_s$ and $d\beta$ as a function of φ_s . To begin, we write $\cos\theta_s$ as follows:

$$\cos\theta_s = \frac{L}{PD} = \frac{L}{[L^2 + \rho_s^2]^{\frac{1}{2}}} \quad (7)$$

where

$$\rho_s^2 = r_0^2 + r_m^2 - 2r_0r_m \cos\varphi_s. \quad (7a)$$

In the figure ρ_s and φ_s are equal to OD and $\angle OAD$, respectively. The differential angle $d\beta$ can be written as a

function of φ_s if we note that

$$\tan\beta = \frac{r_m \sin\varphi_s}{r_0 - r_m \cos\varphi_s}.$$

Taking the derivative of $\tan\beta$, we obtain

$$d\beta = \frac{\cos^2\beta}{(r_0 - r_m \cos\varphi_s)^2} (r_0r_m \cos\varphi_s - r_m^2) d\varphi_s. \quad (8)$$

Since $\rho_s \cos\beta = r_0 - r_m \cos\varphi_s$, (8) becomes

$$\begin{aligned} d\beta &= \frac{1}{\rho_s^2} \left(\frac{r_0^2 + r_m^2 - \rho_s^2}{2} - r_m^2 \right) d\varphi_s \\ &= \frac{r_0^2 - r_m^2}{2} \frac{d\varphi_s}{\rho_s^2} \frac{d\varphi_s}{2}. \end{aligned} \quad (9)$$

Inserting (7) and (9) into (6) we have

$$\begin{aligned} \Omega/2 &= \beta_{\max} - L \int_0^{\beta_{\max}} \frac{d\beta}{(L^2 + \rho_s^2)^{\frac{1}{2}}} \\ &= \beta_{\max} - \frac{L}{2} \frac{(r_0^2 - r_m^2)}{(r_0^2 - r_m^2)} \int_{\pi}^0 \frac{d\varphi_s}{\rho_s^2 (L^2 + \rho_s^2)^{\frac{1}{2}}} \\ &\quad + \frac{L}{2} \int_{\pi}^0 \frac{d\varphi_s}{(L^2 + \rho_s^2)^{\frac{1}{2}}}. \end{aligned} \quad (10)$$

In (10) the φ_s integration is taken in the clockwise direction, i.e., from π down towards zero. To put the integrals in standard form we introduce a new variable γ , where $\gamma = (\pi/2) - (\varphi_s/2)$. It will be convenient at this point to write the terms ρ_s^2 and $L^2 + \rho_s^2$ in a somewhat different form. Since

$$\begin{aligned} \cos\varphi_s &= -\cos 2\gamma \\ &= 2 \sin^2\gamma - 1 \end{aligned}$$

we have from Eq. (7a),

$$\begin{aligned} \rho_s^2 &= r_0^2 + r_m^2 - 2r_0r_m(2 \sin^2\gamma - 1) \\ &= (r_0 + r_m)^2 - 4r_0r_m \sin^2\gamma \\ &= (r_0 + r_m)^2 (1 - \alpha^2 \sin^2\gamma) \end{aligned} \quad (11)$$

and

$$\begin{aligned} L^2 + \rho_s^2 &= L^2 + (r_0 + r_m)^2 - 4r_0r_m \sin^2\gamma \\ &= (L^2 + (r_0 + r_m)^2) (1 - k^2 \sin^2\gamma) \\ &= R_{\max}^2 (1 - k^2 \sin^2\gamma). \end{aligned} \quad (12)$$

The constants α^2 , k^2 , R_{\max}^2 equal the following:

$$\begin{aligned} \alpha^2 &= \frac{4r_0r_m}{(r_0 + r_m)^2} \\ k^2 &= \frac{4r_0r_m}{L^2 + (r_0 + r_m)^2} = 1 - \frac{R_1^2}{R_{\max}^2} \\ R_{\max}^2 &= L^2 + (r_0 + r_m)^2 \\ R_1^2 &= L^2 + (r_0 - r_m)^2. \end{aligned}$$

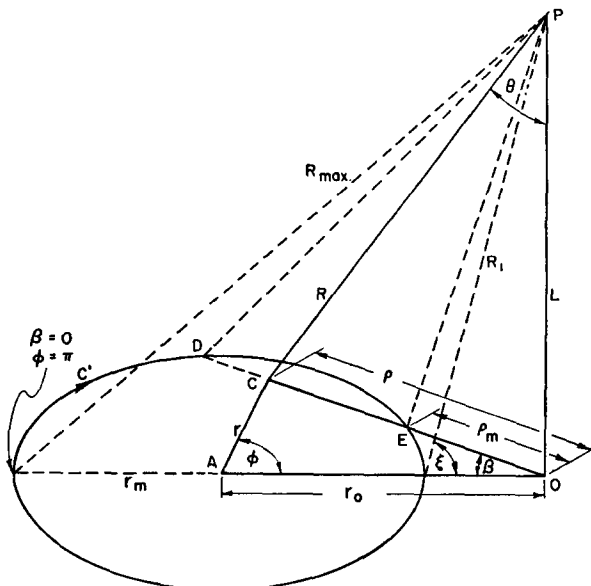


FIG. 2. Solid angle subtended at points outside disk boundary ($r_0 > r_m$).

Inserting (11) and (12) into (10), and making use of the fact that $d\varphi_s = -2d\gamma$, there is obtained

$$\Omega/2 = \beta_{\max} - \frac{L}{R_{\max}} \int_0^{\pi/2} \frac{d\gamma}{(1-k^2 \sin^2 \gamma)^{3/2}} + \frac{L}{R_{\max}} \frac{r_0 - r_m}{r_0 + r_m} \int_0^{\pi/2} \frac{d\gamma}{(1-\alpha^2 \sin^2 \gamma)(1-k^2 \sin^2 \gamma)^{3/2}} \quad (13)$$

The integrals are Legendre's form of the complete elliptic integrals of the first and third kind, designated by $K(k)$ and $\Pi(\alpha^2, k)$, respectively. Therefore, (13) becomes

$$\Omega/2 = \beta_{\max} - \frac{L}{R_{\max}} K(k) + \frac{L}{R_{\max}} \frac{r_0 - r_m}{r_0 + r_m} \Pi(\alpha^2, k)$$

or

$$\Omega = 2\beta_{\max} - \frac{2L}{R_{\max}} K(k) + \frac{2L}{R_{\max}} \frac{r_0 - r_m}{r_0 + r_m} \Pi(\alpha^2, k). \quad (14)$$

The solid angle can be written down directly from (14) for point P at $r_0 = r_m$. We have

$$\begin{aligned} \Omega &= 2\beta_{\max} - \frac{2L}{R_{\max}} K(k) \\ &= \pi - \frac{2L}{R_{\max}} K(k). \end{aligned} \quad (15)$$

Equation (14) can be simplified by writing $\Pi(\alpha^2, k)$ in terms of Heuman's lambda function, Λ_0 . From page 228 of Byrd and Friedman,⁵ we find that $\Pi(\alpha^2, k)$ can be written as follows:

$$\Pi(\alpha^2, k) = \frac{\pi}{2} \frac{\alpha \Lambda_0(\xi, k)}{[(\alpha^2 - k^2)(1 - \alpha^2)]^{1/2}} \quad (16)$$

where

$$\Lambda_0(\xi, k) = \frac{2}{\pi} [E(k)F(\xi, k') + K(k)E(\xi, k') - K(k)F(\xi, k')]$$

$$\xi = \arcsin \left(\frac{1 - k^2/\alpha^2}{1 - k^2} \right)^{1/2} \quad (17)$$

$$k' = (1 - k^2)^{1/2}$$

$$k^2 \leq \alpha^2 < 1.$$

Substituting the expressions for α^2 and k^2 into (16) and (17) we have

$$\begin{aligned} \Pi(\alpha^2, k) &= \pm \frac{\pi}{2} \frac{R_{\max}}{L} \frac{r_0 + r_m}{r_0 - r_m} \Lambda_0(\xi, k) \\ \xi &= \arcsin \frac{L}{R_1} = \arcsin \frac{L}{|r_0 - r_m|}. \end{aligned} \quad (18)$$

⁵ P. F. Byrd and M. C. Friedman, *Handbook of Elliptic Integrals for Engineers and Physicists* (Springer-Verlag, Berlin, 1954).

In applying (18), since $|r_0 - r_m|$ must be used, a (+) sign is used for $r_0 > r_m$ and a (-) sign for $r_0 < r_m$. Inserting (18) into (14), and remembering that $\beta_{\max} = \pi$, we obtain, for $r_0 < r_m$,

$$\Omega = 2\pi - \frac{2L}{R_{\max}} K(k) - \pi \Lambda_0(\xi, k) \quad (19)$$

which is the desired expression. For the special case $r_0 = 0$, $k = 0$, and $\Lambda_0(\xi, 0) = (L/R_1) = (L/R_{\max})$, $K(0) = (\pi/2)$. Therefore, from (19), the solid angle is

$$\begin{aligned} \Omega &= 2\pi - \frac{2L}{R_{\max}} K(0) - \pi \Lambda_0(\xi, 0) \\ &= 2\pi - \frac{\pi L}{R_{\max}} - \frac{\pi L}{R_{\max}} \\ &= 2\pi \left(1 - \frac{L}{R_{\max}} \right) \end{aligned}$$

which is the familiar expression for a point over the center of a circle.

Case II: $r_0 > r_m$

Rewriting Eq. (5) for convenience we have

$$\Omega/2 = \int \int_{\Omega_c'} \sin \theta d\theta d\beta.$$

By inspection of Fig. 2, it will become evident that the limits of θ and β are $\theta_m = \angle OPE$, $\theta_s = \angle OPD$, and $0 \leq \beta \leq \arcsin r_m/r_0$. Therefore, (5) becomes

$$\begin{aligned} \Omega/2 &= \int_0^{\arcsin r_m/r_0} \int_{\theta_m}^{\theta_s} \sin \theta d\theta d\beta \\ &= \int_0^{\arcsin r_m/r_0} [-\cos \theta]_{\theta_m}^{\theta_s} d\beta \\ &= \int_0^{\arcsin r_m/r_0} \cos \theta_m d\beta - \int_0^{\arcsin r_m/r_0} \cos \theta_s d\beta. \end{aligned} \quad (20)$$

Analogous to Case I, $\cos \theta_m$ can be written as follows

$$\cos \theta_m = \frac{L}{PE} = \frac{L}{(L^2 + \rho_m^2)^{1/2}} \quad (21)$$

where $\rho_m = OE$. The term $\cos \theta_s$ is again given by Eq. (7), and as previously $\rho_s = OD$. Inserting (21) and (7) into (20) there is obtained

$$\Omega/2 = L \int_0^{\arcsin r_m/r_0} \frac{d\beta}{(L^2 + \rho_m^2)^{1/2}} - L \int_0^{\arcsin r_m/r_0} \frac{d\beta}{(L^2 + \rho_s^2)^{1/2}} \quad (22)$$

TABLE I. Values of the solid angle for various values of r_0/r_m and L/r_m .

r_0/r_m	$L/r_m=0.5$		$L/r_m=1$		$L/r_m=1.5$		$L/r_m=2$	
	Ω	Ω^a	Ω	Ω^a	Ω	Ω^a	Ω	Ω^a
0	3.4732594		1.8403024		1.0552591		0.6633335	
0.2	3.4184435	3.41844	1.8070933	1.80709	1.0405177	1.04052	0.6566352	0.656633
0.4	3.2435434	3.24354	1.7089486	1.70895	0.9975504	0.997549	0.6370508	0.637049
0.6	2.9185178	2.91852	1.5517370	1.55174	0.9301028	0.930101	0.6060694	0.606068
0.8	2.4122535	2.41225	1.3488367	1.34883	0.8441578	0.844152	0.5659755	0.565969
1	1.7687239	1.76872	1.1226876	1.12269	0.7472299	0.747229	0.5195359	0.519535
1.2	1.1661307	1.16614	0.9003572	0.900369	0.6472056	0.647217	0.4696858	0.469697
1.4	0.7428889	0.742893	0.7039130	0.703917	0.5509617	0.550965	0.4191714	0.419175
1.6	0.4841273	0.484130	0.5436956	0.543705	0.4632819	0.463285	0.3702014	0.370204
1.8	0.3287007	0.328702	0.4195415	0.419543	0.3866757	0.386678	0.3243908	0.324392
2	0.2324189	0.232420	0.3257993	0.325801	0.3217142	0.321716	0.282707	0.282709

^a See reference 6.

Referring to Fig. 2, it is evident that ρ_m^2 bears the same relationship to φ_s as ρ_s^2 , and is therefore equal to (7a), the difference being that the limits of φ_s are different for each. In this case φ_s is double valued having the values $\angle OAD$ and $\angle OAE$, respectively, as β goes from zero to arc $\sin r_m/r_0$. Since ρ_m^2 , ρ_s^2 , and $d\beta$ are functions of φ_s only (for fixed L , r_0 , r_m) as can be seen from Eqs. (7a) and (9), and since ρ_m and ρ_s are the same function of ϕ_s , (22) can be written as follows

$$\Omega/2 = \int_0^{\varphi_T} f(\varphi_s) d\varphi_s - \int_{\pi}^{\varphi_T} f(\varphi_s) d\varphi_s \quad (23)$$

where φ_T is the value of φ_s at the tangent point and is equal to arc $\cos r_m/r_0$. In (23) $f(\varphi_s) d\varphi_s$ has been set equal to the following:

$$f(\varphi_s) d\varphi_s = \frac{L d\beta}{(L^2 + \rho_m^2)^{3/2}}, \quad \frac{L d\beta}{(L^2 + \rho_s^2)^{3/2}} \quad (24)$$

Equation (23) as it stands does not lend itself readily to solution. A more tractable equation can be obtained as follows. Noting that

$$\int_0^{\varphi_T} f(\varphi_s) d\varphi_s = - \int_{\varphi_T}^0 f(\varphi_s) d\varphi_s$$

and

$$\int_{\pi}^{\varphi_T} f(\varphi_s) d\varphi_s + \int_{\varphi_T}^0 f(\varphi_s) d\varphi_s = \int_{\pi}^0 f(\varphi_s) d\varphi_s$$

(23) becomes

$$\begin{aligned} \Omega/2 &= - \int_{\varphi_T}^0 f(\varphi_s) d\varphi_s - \int_{\pi}^{\varphi_T} f(\varphi_s) d\varphi_s \\ &= - \int_{\pi}^0 f(\varphi_s) d\varphi_s. \end{aligned} \quad (25)$$

Using (24), (9), and (7a), Eq. (25) takes the following

form:

$$\Omega/2 = + \frac{L}{2} \int_{\pi}^0 \frac{d\varphi_s}{(L^2 + \rho_s^2)^{3/2}} - \frac{L(r_0^2 - r_m^2)}{2} \int_{\pi}^0 \frac{d\varphi_s}{\rho_s^2 (L^2 + \rho_s^2)^{3/2}} \quad (26)$$

The integrals in (26) are the same as those in (10), and have therefore been evaluated. Comparing (10) and (14), (26) becomes

$$\Omega/2 = - \frac{L}{R_{\max}} K(k) + \frac{L}{R_{\max}} \frac{r_0 - r_m}{r_0 + r_m} \Pi(\alpha^2, k)$$

or

$$\Omega = - \frac{2L}{R_{\max}} K(k) + \frac{2L}{R_{\max}} \frac{r_0 - r_m}{r_0 + r_m} \Pi(\alpha^2, k). \quad (27)$$

Writing $\Pi(\alpha^2, k)$ in terms of Heuman's lambda function, we have

$$\Omega = - \frac{2L}{R_{\max}} K(k) + \pi \Lambda_0(\xi, k). \quad (28)$$

IV. SUMMARY OF RESULTS

To summarize, the following equations have been derived.

$$\begin{aligned} \Omega &= 2\pi - \frac{2L}{R_{\max}} K(k) - \pi \Lambda_0(\xi, k) & r_0 < r_m \\ &= \pi - \frac{2L}{R_{\max}} K(k) & r_0 = r_m \\ &= - \frac{2L}{R_{\max}} K(k) + \pi \Lambda_0(\xi, k) & r_0 > r_m. \end{aligned}$$

Using the foregoing equations, Table I was prepared in which the solid angle is given for several values of r_0/r_m and L/r_m . Values of the solid angle taken from Masket *et al.*⁶ are included for comparison.

⁶ Masket, Macklin, and Schmitt, "Tables of solid angles and activations," ORNL-2170 (Oak Ridge National Laboratory, Oak Ridge, Tennessee, November, 1956).

In determining the solid angle subtended at an arbitrary point, one must determine the functions $K(k)$ and $\Lambda_0(\xi, k)$. Usually this involves computing arc $\sin k$, and for Λ_0 , the additional parameter ξ . The tables⁷ in reference 4 give values of $K(k)$ and $\Lambda_0(\xi, k)$ for a one degree difference in arc $\sin k$ and ξ between 0 and $\pi/2$. For fractions of a degree, interpolation to obtain $\Lambda_0(\xi, k)$ is more involved than for $K(k)$ since there are two parameters to consider; however, the calculation is straightforward.

⁷ A short table of $\Lambda_0(\xi, k)$ is also given in reference 5.

The method which has been described for obtaining the solid angle appears to have some advantages over the series method mentioned in the introduction since with the availability of the tables, one essentially has to find the desired $K(k)$ and $\Lambda_0(\xi, k)$ which usually is not difficult within the limits of engineering accuracy. Also, in the series expansion, the series will converge more or less rapidly depending on the values of α^2 and k^2 ; therefore, the calculation might become tedious.

Vacuum-Type Gas-Flow Calibrator*

WILLIAM A. STRAUSS AND RUDOLPH EDSE

Department of Aeronautical Engineering, The Ohio State University, Columbus 10, Ohio

(Received October 9, 1958; and in final form, January 12, 1959)

A vacuum-type gas-flow calibrator was designed and constructed for making accurate calibrations of flowmeters needed for the investigation of high-pressure flames. This calibrator operates by automatically measuring the time required to pressurize a known volume from a near vacuum to 1 atmosphere pressure. The gas volume flow rate is obtained by dividing the calibration volume by the pressurization time and applying corrections from PVT data. This apparatus has been successfully used to calibrate flowmeters for use with hydrogen, oxygen, nitrogen, air, methane, nitric oxide, carbon monoxide, and various homogeneous nonexplosive gas mixtures.

INTRODUCTION

THE basic principle of operation of the vacuum calibration unit is to measure the time required to pressurize a container of known volume from a near vacuum to 1 atmosphere with a constant flow of gas from a flowmeter (see appendix). The volume flow per unit time (\dot{v}) may then be computed by simply dividing the volume of the reservoir (V) by the time required to raise the pressure in the containers to one atmosphere (t), or

$$\dot{v} = \frac{V}{t}$$

The volume flow may then be corrected to standard temperature and pressure conditions (\dot{v}_0) by the equation of state relationship. Hence,

$$\dot{v}_0 = \frac{V}{t} \frac{\Delta p}{p_0} \frac{T_0}{T}$$

where p_0 = standard pressure (760 mm Hg), Δp = pressure rise (mm Hg), T_0 = standard temperature (273°K), T = gas temperature (°K). It is understood that this approach yields reliable results only when the perfect gas assumption is justified. Otherwise PVT corrections must be applied.

The calibration of gas flowmeters by the vacuum calibration method has the advantage over the water displacement method that no water vapor corrections are needed and that no errors are introduced due to absorption of the calibrated gas by the water.

APPARATUS

Figure 1 is a flow diagram of the vacuum calibration unit apparatus. It consists basically of 4 reservoirs of known volumes, a back-pressure regulator, a U-tube mercury manometer, a series of plug valves to control the direction of the gas flow and 4 solenoid actuated valves. Gas from the flowmeter being calibrated is introduced into the vacuum calibrator through a 3-way solenoid valve (valve D) only when the valve is actuated. Otherwise, the constant flow of gas is exhausted to the atmosphere. Valve A is a safety valve which is actuated by a pressure switch to prevent accidental over-pressurization of the calibration unit reservoirs. The back-pressure regulator is located immediately upstream from the vacuum calibration unit solenoid valve D . It maintains a constant pressure of approximately 10 psig on the downstream side of the throttle valve and prevents flow variations due to varying pressure drop across the throttle valve. The electrical circuitry of the solenoid valves B , C , and D , is such that when one is energized, it is not possible to actuate either of the other two until the first has been de-energized.

* The flame-study work was supported by Wright Air Development Center Aeronautical Research Laboratory under Contract AF 33(616)-5439.